Oxygen K-edge x-ray absorption near-edge structure in crystalline and amorphous molybdenum trioxides

2004 J. Phys.: Condens. Matter 16 6619

(http://iopscience.iop.org/0953-8984/16/36/027)

INSTITUTE OF PHYSICS PUBLISHING JOURNAL OF PHYSICS: CONDENSED MATTER

J. Phys.: Condens. Matter **16** (2004) 6619–6625 PII: S0953-8984(04)81979-9

Oxygen K-edge x-ray absorption near-edge structure in crystalline and amorphous molybdenum trioxides

J Gaidelene[1], **A Kuzmin**[1,3] **and J Purans**[1,2]

[1] Institute of Solid State Physics, University of Latvia, Kengaraga street 8, LV-1063 Riga, Latvia
[2] Dipartimento di Fisica dell'Università di Trento, via Sommarive 14, I-38050 Povo (Trento), Italy

E-mail: a.kuzmin@cfi.lu.lv

Received 11 June 2004, in final form 11 June 2004
Published 27 August 2004
Online at stacks.iop.org/JPhysCM/16/6619
doi:10.1088/0953-8984/16/36/027

Abstract

X-ray absorption near-edge structure (XANES) signals at the oxygen K edge in polycrystalline α-MoO_3 and amorphous a-MoO_3 thin film were analysed within the full-multiple-scattering (FMS) formalism. Significantly different XANES signals were found for non-equivalent oxygen atoms in low-symmetry layered-type α-MoO_3 structure. The obtained results are in agreement with the experimental data and allow us to interpret all XANES peaks for α-MoO_3. Besides, the FMS XANES simulations, performed for several fragments of α-MoO_3 structure, allowed us to explain the O K-edge XANES in amorphous a-MoO_3 thin film. We found that although the crystallographic structures of α-MoO_3 and a-MoO_3 are strongly different, a cluster consisting of six MoO_6 octahedra joined by vertices produces the main contribution to both XANES signals.

1. Introduction

Molybdenum trioxide (MoO_3) is an important technological material, which is used as a heterogeneous catalyst component [1], in electro/photochromic devices [2] and in ion beam resist applications [3]. At ambient conditions, crystalline molybdenum trioxide exists in two polymorphs: ReO_3-type meta-stable monoclinic β-MoO_3 [4] and layered orthorhombic α-MoO_3 [5]. The latter phase will be addressed in the present work.

Molybdenum oxide can be also prepared as a thin film using several experimental techniques [6]. These include thermal evaporation, rf sputtering and dc reactive magnetron sputtering, electron gun, chemical vapour and pulsed laser deposition, sol–gel technology and electrodeposition from solutions [6]. Depending on the experimental conditions and post-preparation treatment, both amorphous and crystalline films can be obtained.

[3] Author to whom any correspondence should be addressed.

Table 1. Structural parameters of orthorhombic α-MoO_3 from [5] used in the XANES calculations. The space group is $Pbnm$; the lattice parameters are $a = 3.963$ Å, $b = 13.855$ Å and $c = 3.696$ Å.

Atom	Wyckoff position	x	y	z
Mo	(4c)	0.0867	0.1016	0.2500
O(1)	(4c)	0.4994	0.4351	0.2500
O(2)	(4c)	0.5212	0.0886	0.2500
O(3)	(4c)	0.0373	0.2214	0.2500

The α-MoO_3 structure (figure 1 and table 1) is composed of highly distorted MoO_6 octahedra joined in the c-axis direction by vertices and edges to form double zigzag chains and in the perpendicular a-axis direction only by vertices [5]. The layers are separated one from another in the b-axis direction by 3 Å. Strong distortion of MoO_6 octahedra results in a different type of the Mo–O bonding. The oxygen atoms in the octahedron can be divided into three groups [5]: non-bridging (Mo=O double bond, R(Mo–O) = 1.67 Å), bridging between two molybdenum atoms along the a-axis (Mo–O–Mo, R(Mo–O) = 1.73 and 2.25 Å) and bridging between three molybdenum atoms in the bc-plane (R(Mo–O) = 1.95, 1.95 and 2.33 Å).

The atomic structure of amorphous molybdenum oxide (a-MoO_3) is less clear. It is believed that it is built from corner-sharing MoO_6 octahedra [7]. This conclusion was supported by our previous extended x-ray absorption fine-structure (EXAFS) studies at the Mo K edge [8–11], which also suggested strong distortion of MoO_6 octahedra.

The investigation of the oxygen K edge in molybdenum oxide can provide us with complementary information on the Mo–O bonding, since the O K edge has much better resolution and is more sensitive to the covalency effects. The O K edge has been experimentally studied in α-MoO_3 [12–17] and a-MoO_3 [12], but only qualitative interpretation of the peaks in x-ray absorption near-edge structure (XANES) signals has been given in previous works.

In this work we present results of theoretical *ab initio* full-multiple-scattering (FMS) XANES simulations, which allowed us to explain all features in the O K-edge x-ray absorption spectra in crystalline α-MoO_3 and amorphous a-MoO_3 thin film.

2. Experimental and data analysis

The experimental spectra of the O K edge in α-MoO_3 and a-MoO_3 as well as experimental details have been published by us previously [17]. Note that our spectrum for α-MoO_3 [17] has better resolution than that published previously in [12–15] for powder samples and is comparable in resolution with polarization dependent measurements on α-MoO_3 single crystals [16].

The O K-edge XANES signals were analysed qualitatively by a comparison of experimental data with theoretical spectra (figure 2) calculated by the FEFF8 code [18] within the FMS approach. Due to the low crystallographic symmetry of α-MoO_3 (figure 1), there are three non-equivalent oxygen atoms (table 1), whose XANES signals were calculated separately. Thus, three different clusters, having the crystallographic structure of α-MoO_3 [5], were constructed around each non-equivalent oxygen atom with the maximum radius equal to 10 Å. They included up to 338 atoms. Calculations of the cluster potentials were done in the muffin-tin self-consistent-field (SCF) approximation. The self-consistency was achieved for smaller cluster sizes of about 4 Å around the absorber. The complex Hedin–Lundqvist potential [19, 20] was used to approximate exchange and correlation effects. The O K-edge core-hole level width was set to 0.16 eV [19]. The FMS calculations were done for several cluster sizes.

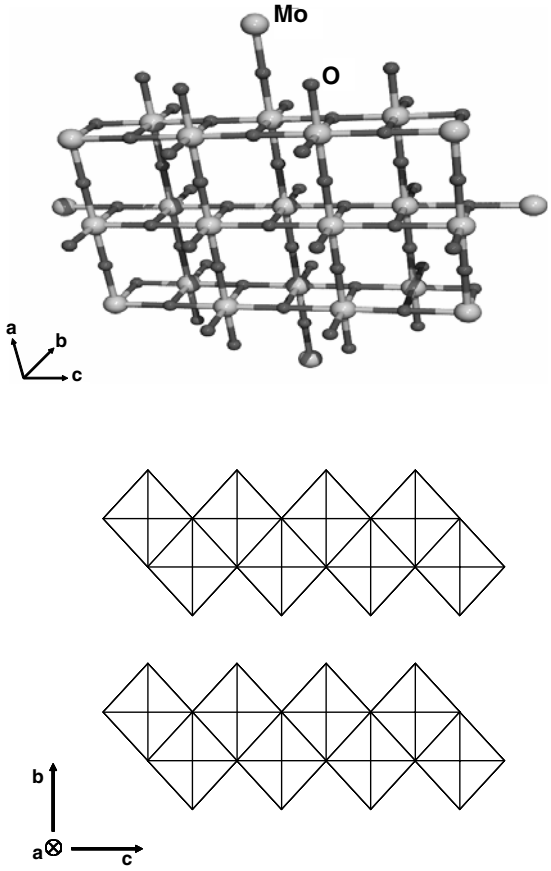

Figure 1. (a) Schematic representation of the idealized structure of α-MoO_3. (b) The layer in α-MoO_3 structure. Large light spheres are molybdenum atoms; small dark spheres are oxygen atoms.

We have also performed calculations for several model clusters (see below), built from regular MoO_6 octahedra with R(Mo–O) $=$ 1.95 Å and representing characteristic parts of α-MoO_3 crystallographic structure.

3. Results and discussion

The calculated XANES signals are compared to the experimental one in figure 2, where results are shown separately for each non-equivalent oxygen atom. The obtained agreement is rather good and allows us to interpret qualitatively all features present in the experiment. The main observed difference is related to a mismatch of the energy scale, resulting in the features in the calculated spectra appearing progressively at lower energies than in the experiment. Such a difference is presumably due to inaccuracies in the calculation of the cluster potential, mainly the exchange and correlation part. Note that it can be, in principle, compensated by a multiplication of the energy scale for the theoretical data by an *ad hoc* constant around 1.18. The correspondence between features in the calculated and experimental spectra, due to such an energy scale correction, is shown in figure 2 by arrows.

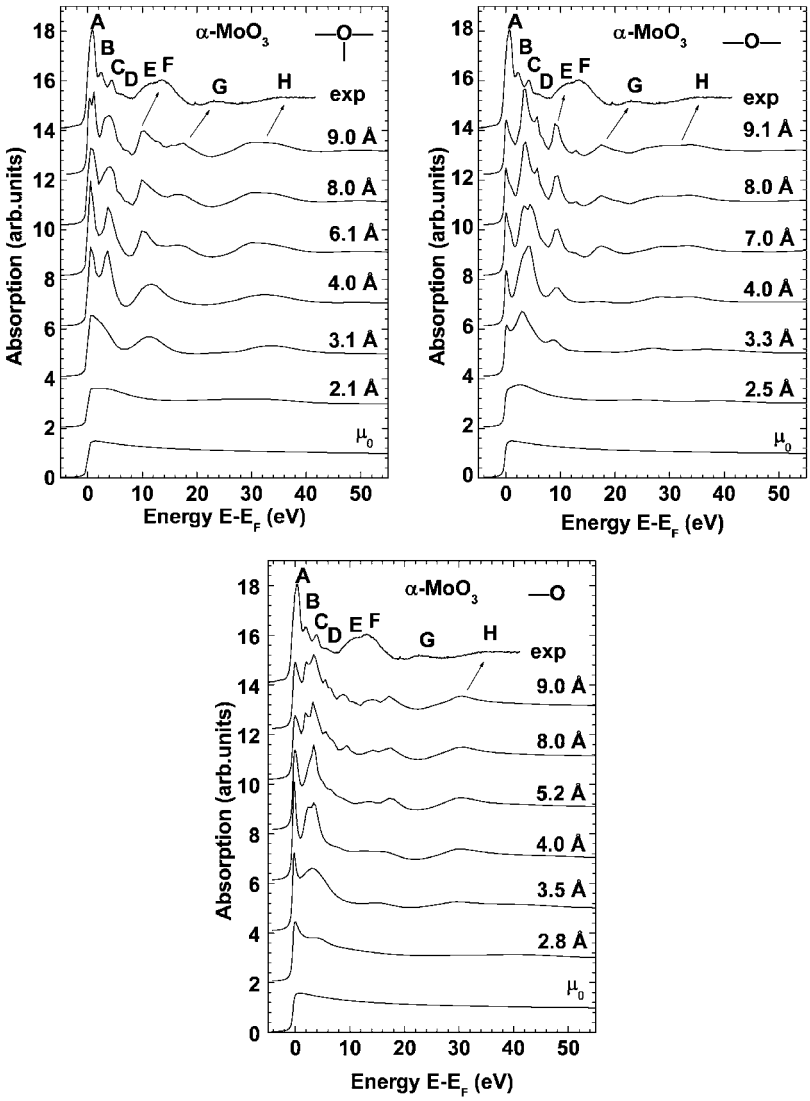

Figure 2. Experimental (upper curve) and calculated O K-edge XANES signals in α-MoO_3. Upper left panel: for bridging oxygens O(1) along the *c*-axis. Upper right panel: for bridging oxygens O(2) along the *a*-axis. Lower panel: for non-bridging oxygen O(3). E_F is the Fermi level.

The low symmetry of the α-MoO_3 structure results in many non-equivalent scattering paths contributing to the total XANES signal. Therefore, an increase of the cluster size around the absorbing oxygen atoms leads to the appearance of fine structure, being the result of a complex interference effect. This makes the detailed interpretation complicated; however, the origin of the main features observed in the experimental XANES can be explained by the calculation. All features in figure 2 observed in the experiment and labelled, according to [17], by letters from A to H are reproduced by the FMS calculations for the cluster size of around 7–8 Å. Note that addition of shells composed of oxygen atoms makes a larger contribution to the total XANES signal compared to shells consisting of molybdenum atoms. This is because the scattering amplitude of oxygen has larger intensity close to the Fermi level.

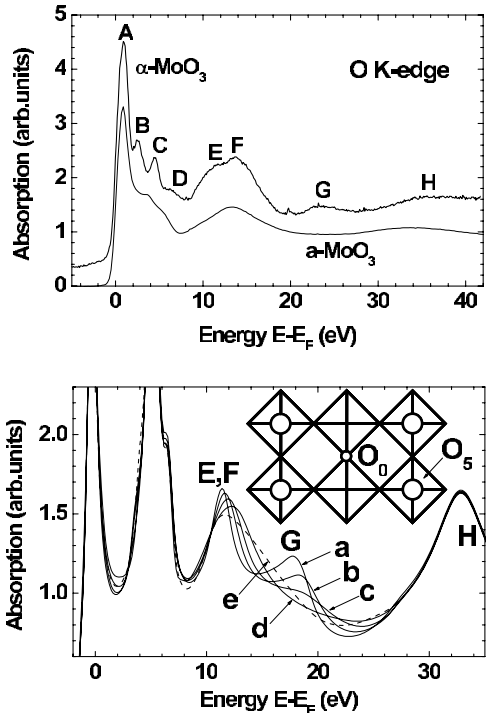

Figure 3. Upper panel: oxygen K-edge XANES spectra in polycrystalline α-MoO_3 and amorphous a-MoO_3 thin film. Lower panel: theoretically calculated O K-edge XANES signals for the cluster of six MoO_6 octahedra (R(Mo–O) = 1.95 Å), lying in plane and joined by vertices. O_0 is the central absorbing oxygen atom; O_5 is the one of eight oxygen atoms located in the fifth coordination shell of O_0. The XANES signals correspond to the clusters with oxygen atoms O_5 displaced in a random direction by (a) 0 Å; (b) 0.3 Å; (c) 0.5 Å; (d) 0.8 Å and (e) without O_5 oxygen atoms (shown by dashed curve for clarity).

All three non-equivalent oxygen atoms are responsible for the first four features A–D. These peaks were interpreted previously [13–17] as transitions from the 1s(O) core state to strongly hybridized 2p(O)–4d(Mo) states. The octahedral crystal field splits the 4d(Mo) band into t_{2g} and e_g sub-bands, and the distortion of octahedra in α-MoO_3 leads to further splitting of the t_{2g} and e_g states into A, B and C, D components, respectively.

The next group of peaks E–H were not interpreted in [13–16]. We attributed [17] these peaks to the 5sp(Mo)–2p(O) states and to the scattering resonances at the nearest atoms. Present results suggest that peaks E, F and H appear in the XANES for clusters consisting of at least two coordination shells. However, peaks E and F are mainly due to bridging oxygen atoms, whereas peak H is due to all oxygen atoms.

The origin of peak G represents the most interest. In theoretical XANES spectra for α-MoO_3, this peak is the most prominent in the signals of bridging oxygen atoms. At the same time, peak G is completely absent in amorphous a-MoO_3 thin film (figure 3). Note also that peak G exists in perovskite-type compounds as ReO_3, Na_xWO_3 and WO_3, where its intensity changes a lot depending on the compound symmetry and disorder present [17, 21]. To understand the origin of peak G, we performed a number of model simulations using different clusters, which resemble parts of the real α-MoO_3 and perovskite-type structures. Note that the layer in α-MoO_3 can be considered as two perovskite-type layers joined by edges.

The model, which explains the origin of peak G, is shown in figure 3. It consists of six MoO_6 octahedra lying in plane and joined by vertices as in a perovskite-type layer with the Mo–O–Mo angles equal to 180°. Note that due to the simplicity of the model the obtained theoretical XANES signals (lower panel in figure 3) differ quantitatively from the experimental ones (upper panel in figure 3); nevertheless, the model allows us to understand the qualitative origin of the XANES features. In our model cluster, the central absorbing oxygen atom is denoted as O_0 and the eight oxygen atoms located in the fifth shell are denoted as O_5. When O_5 atoms are not displaced, peak G is very intense (curve (a) in figure 3). A displacement of O_5 atoms in random directions leads to a distortion of MoO_6 octahedra and a decrease of the peak G intensity. The intensity lowering correlates with an amount of O_5 atom displacement, so that their shift by 0.8 Å (curve (e) in figure 3) results in a complete disappearance of peak G. Therefore, the intensity of peak G can be used as a fingerprint of the particular distortion occurring in the group of octahedra, joined as in perovskite-type layers. This fact can be useful in the O K-edge studies of structural phase transitions in perovskites.

Now we turn to the O K-edge XANES in amorphous a-MoO_3 thin film (see the upper panel in figure 3). It resembles closely the signal for polycrystalline α-MoO_3 with two principal differences. First, the features A–F decrease their intensity, so that peak B is not visible at all, and peaks C and E become much weaker. Second, feature G is completely absent. Our previous Mo K-edge EXAFS and XANES studies of a-MoO_3 thin films [8–11] indicate that their local structure is composed of distorted MoO_6 octahedra joined by vertices, and, thus, is more similar to the structure of perovskite-type β-MoO_3 [22] and β'-MoO_3 [23, 24] than of α-MoO_3 [5]. The distortion of MoO_6 octahedra in a-MoO_3 is such that a group of four nearest oxygen atoms are bound to the molybdenum atom much more strongly than the remaining two oxygens [10, 11]. The difference in the distortion of MoO_6 octahedra in a-MoO_3 and α-MoO_3 leads to a difference in the crystal field splitting of the 4d(Mo) states and in a change of 2p(O)–4d(Mo) interaction. The latter fact is responsible for a decrease of the feature A–D intensity in a-MoO_3 that can be related to an increase of the ionicity (molybdenum-to-oxygen charge transfer [25]) of the Mo–O bonds [17]. Such a conclusion allows us to explain the origin of structural disorder in a-MoO_3 as due to the weaker Mo–O bonds, which lead to a larger variation of Mo–O–Mo angles between adjacent coordination polyhedra.

The absence of peak G in amorphous a-MoO_3 thin film (lower panel in figure 3) allows us to estimate the size of the structural region which is rather well ordered. The distance between two oxygen atoms, O_0 and O_5, is about 4.8 Å. This value corresponds to the distance in the Fourier transform (FT) of the Mo K-edge EXAFS spectrum (see figure 2 in [9]), at which no well defined peaks can be observed (note that in the FT the positions of the peaks are shifted to lower distances by 0.3–0.5 Å due to the presence of the backscattering phase in the EXAFS function).

4. Conclusions

The analysis of the O K-edge XANES in polycrystalline orthorhombic α-MoO_3 and amorphous a-MoO_3 thin film was performed within the full-multiple-scattering (FMS) formalism. The FMS calculations for α-MoO_3 were done using a set of clusters with a size up to 10 Å. Significantly different XANES signals were found for non-equivalent oxygen atoms in low-symmetry layered-type α-MoO_3 structure. The obtained results are in agreement with the experimental data and allow us to interpret all XANES features for α-MoO_3.

Besides, FMS XANES simulations, performed for several fragments of α-MoO_3 structure, allowed us to explain the O K-edge XANES for amorphous a-MoO_3 thin film. We found that although the crystallographic structures of α-MoO_3 and a-MoO_3 are very different, a cluster

consisting of six MoO_6 octahedra joined by vertices produces the main contribution to both XANES signals. This result provides us with a fingerprint (the presence or absence of feature G in figure 3), which is useful for the interpretation of perovskite-type systems.

Acknowledgments

We thank the LURE (Orsay, France) SUPER ACO SA22 beam-line staff Dr Ph Parent and Dr C Laffon for their technical collaboration. This work was partially supported by the Latvian government grants 1.0811 and 1.0821.

References

[1] Haber J and Lalik E 1997 *Catal. Today* **33** 119
[2] Li Y M and Kudo T 1995 *Sol. Energy Mater. Sol. Cells* **39** 179
[3] Hashimoto M, Koreeda T, Koshida N, Komuro M and Nobufumi A 1998 *J. Vac. Sci. Technol.* B **16** 2767
[4] Harb F, Gerand B, Nowogrocki G and Figlarz M 1989 *Solid State Ion.* **32/33** 84
[5] Kihlborg L 1963 *Ark. Kemi* **21** 357
[6] He T and Yao J 2003 *J. Photochem. Photobiol.* C **4** 125
[7] Granqvist C G 1995 *Handbook of Inorganic Electrochromic Materials* (Amsterdam: Elsevier)
[8] Balerna A, Bernieri E, Burattini E, Lusis A, Kuzmin A, Purans J and Cikmach P 1991 *Nucl. Instrum. Methods* A **308** 234
[9] Burattini E, Purans J and Kuzmin A 1993 *Japan. J. Appl. Phys.* **32** (Suppl. 32-2) 655
[10] Kuzmin A and Purans J 1997 *J. Physique Coll.* IV **7** C2 971
[11] Kuzmin A and Purans J 1997 *Proc. SPIE* **2968** 180
[12] Mountjoy G, Yuan J and Gaskell P H 1993 *Inst. Phys. Conf. Ser.* **138** 35
[13] Duda L C, Guo J H, Nordgren J, Stagarescu C B, Smith K E, McCarroll W, Ramanujachary K and Greenblatt M 1997 *Phys. Rev.* B **56** 1284
[14] Chen J G 1998 *Catal. Today* **43** 147
[15] Rodriguez J A, Hanson J C, Chaturvedi S, Maiti A and Brito J L 2000 *J. Chem. Phys.* **112** 935
[16] Sing M, Neudert R, von Lips H, Golden M S, Knupfer M, Fink J, Claessen R, Mücke J, Schmitt H, Hüfner S, Lommel B, Aßmus W, Jung Ch and Hellwig C 1999 *Phys. Rev.* B **60** 8559
[17] Purans J, Kuzmin A, Parent Ph and Laffon C 2001 *Electrochim. Acta* **46** 1973
[18] Ankudinov A L, Ravel B, Rehr J J and Conradson S D 1998 *Phys. Rev.* B **58** 7565
[19] Rehr J J, Mustre de Leon J, Zabinsky S I and Albers R C 1991 *J. Am. Chem. Soc.* **113** 5135
[20] Mustre de Leon J, Rehr J J, Zabinsky S I and Albers R C 1991 *Phys. Rev.* B **44** 4146
[21] Purans J, Kuzmin A, Parent Ph and Laffon C 1999 *Physica* B **259–261** 1157
[22] Parise J B, McCarron E M III, Von Dreele R and Goldstone J A 1991 *J. Solid State Chem.* **93** 193
[23] Parise J B, McCarron E M III, Sleight A W and Prince E 1988 *Mater. Sci. Forum* **27** 85
[24] Parise J B, McCarron E M III and Sleight A W 1987 *Mater. Res. Bull.* **22** 803
[25] de Groot F M F, Grioni M, Fuggle J C, Ghijsen J, Sawatzky G A and Petersen H 1989 *Phys. Rev.* B **40** 5715